Peer-reviewed version available at Nanomaterials 2019, 9, 554; doi:10.3390/nano9040554

Microscopic views of atomic and molecular oxygen bonding with *epi* Ge(001)-2×1 studied by high-resolution synchrotron radiation photoemission

Yi-Ting Cheng [1], Hsien-Wen Wan [1] Chiu-Ping Cheng [2]*, Jueinai Kwo [3]*, Minghwei Hong [1]*, and Tun-Wen Pi [4,]*

[1] Graduate Institute of Applied Physics and Department of Physics, National Taiwan University, Taipei, Taiwan, 10617, R.O.C.; ceo6120@gmail.com (Y.-T.C.); b00202022@ntu.edu.tw (H.-W.W.)
[2] Department of Electrophysics, National Chiayi University, Chiayi, Taiwan 60004, R.O.C.;
[3] Department of Physics, National Tsing Hua University, Hsinchu, Taiwan 30013, R.O.C.;
[4] National Synchrotron Radiation Research Center, Hsinchu, Taiwan 30076, R.O.C.

* Correspondence: pi@nsrrc.org.tw (T.-W.P.) (Tel.: +886-3-578-0281), cpcheng@mail.ncyu.edu.tw (C.-P.C.), raynien@phys.nthu.edu.tw (J.K.), mhong@phys.ntu.edu.tw (M.H.)

Abstract:

Embryo stage of oxidation of an *epi* Ge(001)-2×1 by atomic oxygen and molecular O_2 is studied via synchrotron radiation photoemission. The topmost surface buckled with the up- and down-dimer atoms and the first subsurface layer behave distinctly from the bulk by exhibiting surface core-level shifts in the Ge 3d core-level spectrum. The O_2 molecules become dissociated upon reaching the *epi* Ge(001)-2×1 surface. One of the O atom removes off the up-dimer atom, and the other bonds with the underneath Ge atom in the subsurface layer. Atomic oxygen adsorbed on the *epi* Ge(001)-2×1 preferentially in between the up-dimer atoms and the underneath subsurface atoms without affecting the down-dimer atoms. The electronic environment of the O-affiliated Ge up-dimer atoms becomes similar to that of the down-dimer atoms. Both exhibit an enrichment in charge, where the subsurface of the Ge layer is maintained in a charge-deficient state. The dipole moment originally generated in the buckled reconstruction no longer exists, thereby resulting in a decrease in the ionization potential. The down-dimer Ge atoms and the back-bonded subsurface atoms remain inert to atomic O and molecular O_2, a possible cause of low reliability in Ge-related metal-oxide-semiconductor (MOS) devices.

Keywords: Ge(001)-2×1; oxidation; synchrotron radiation photoemission

1. Introduction

Both Ge and III-V compound semiconductors are channel materials to replace silicon in p- and n-type metal-oxide-semiconductor field-effect transistors (MOSFETs) because of their high carrier mobilities [1-10]. For the III-V MOS, the established reports clearly showed that a high-quality oxide/(In)GaAs interface leads to high-performance (In)GaAs MOSFETs in drain currents and transconductances [9-13]. Needless to say, the premise of a high-quality interface requires a III-V surface with high qualities as impurity-free and a long-range order reflecting the nominal surface-atomic structure. Namely, researchers are obligated to grow a high-κ dielectric oxide onto a well-defined reconstructed III-V surface. Years of researches on (In)GaAs(001) have concluded that chemical processes to the hetero-element surfaces would destroy the long-range order; removal of the native oxides is out of the question for attaining a high-quality high-κ/III-V interface. To be specific, the as-grown (In)GaAs surface from a molecular-beam epitaxy (MBE) chamber or a metal organic chemical vapor deposition (MOCVD) reactor must be placed in direct contact with a dielectric oxide prepared with MBE or atomic layer deposition (ALD) without exposing it to air. As to Ge, the

Peer-reviewed version available at Nanomaterials 2019, 9, 554; doi:10.3390/nano9040554

surface pretreatment with assorted chemicals becomes common habits prior to dielectric deposition in the literature. Never a question be asked whether the act is proper or not. The confidence is fully plagiarized from the success of Si, where surface treatments are necessary for further device fabrication. This immediately alerts us in light of the (In)GaAs conclusion that the paused success of Ge MOSFETs is presumably due not to take seriously the surface quality into consideration. Moreover, the engineering and surface-science communities especially the synchrotron-radiation circle have fought wars independently without close communications with each other, further hindering sufficient understandings of the interfaces.

Study of GeO_2/Ge becomes inevitable as a prime topic to desirously obtain an interface similar to that of SiO_2/Si with the oxide downsized to a few atomic layers. Researchers on Ge naturally incline to take the established Si knowledge to propose Ge MOS structure, and intensive researches [14-19] and industry-scale development efforts in the Ge MOS have been undertaken to realize the product. Nevertheless, fundamental researches on Ge is lacking today because the Ge(001)-2×1 surface undergoes similar reconstruction as that of Si(001)-2×1 and the surface and interfacial behaviors of Ge(001)-2×1 are believed to be no differences from those of Si(001)-2×1. Never a question be asked if the move is legitimate. As a matter of fact, the surface electronic structure of Ge(001)-2×1 reveals undeniable difference from that of Si(001)-2×1, where synchrotron radiation photoelectron spectroscopy (SRPES) shows the latter exhibiting distinct surface behavior down to the third layer [20,21], but the former only to the second layer at room temperature [22]. See Fig. 1. Furthermore, Sun *et al*. have demonstrated that the Ge(001) surface becomes noticeably rough after exposure to aqueous HF and HCl solutions [23].

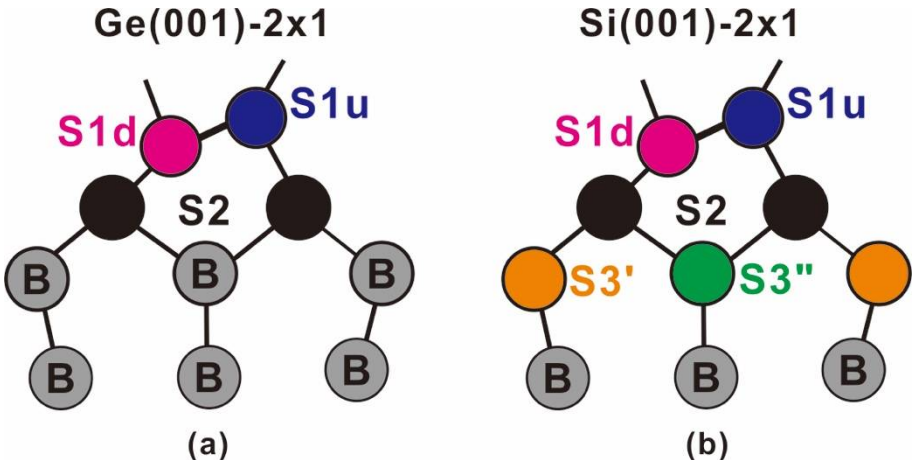

Figure 1. Schematic side-view drawings of **(a)** buckled Ge(001)-2×1 and **(b)** buckled Si(001)-2×1 surface. Symbols S1u, S1d, S2, and S3 stand for the up-dimer atom, down-dimer atom, atoms in the second surface layer, and atoms in the third surface layer, respectively. In Ge(001)-2×1, the S3 atoms show one electronic environment, but in Si(001)-2×1, they are differentiated with S3′ and S3″ electronic environments.

The lack of a detailed understanding of the Ge(001)-2×1 surface deters us from understanding why Ge(001)-2×1 is unlikely to produce 1+ to 4+ charge states as Si(001)-2×1 does [24]. The reported four Ge charge states were commonly observable by neutral beam oxidation [25], through chemically wetted treatments [26], during acid processes [27,28], or upon sudden exposure to a large amount of atomic oxygen on a 2×1 reconstructed surface [29]. It is odd to see that these thick Ge oxides respond differently with heat, one showing an increase [30] and the other a decrease [27] in the strength of GeO_2 with increasing annealing temperatures. Nevertheless, the investigation of a thick Ge oxide film does not help us to fully understand the oxygen-contacted Ge-Ge dimers layer. Other method as *in vacuo* process using supersonic molecular oxygen beams produces only the 1+ and 2+ oxidation states in sub-monolayer thickness [31]. The weak bonding of molecules on Ge(001) [32,33] and confined adsorption site at the surface dimers without insertion into the Ge backbonds [34] have rendered the four charge states unlikely to be formed at the interfacial region of Ge(001). It is worth mentioning

that the growth 1+ to 4+ charge states of Si-oxides occurs by local nucleation [24], which commences from as small as 10 Langmuir (L) of O_2 adsorption on a heated Si sample.

Upon deposition of a high-κ dielectric oxide onto a Ge(001) wafer, O_2 is introduced into the MBE chamber in order to compensate for the loss of oxygen from bombarding the oxide target. The partial pressure of O_2 is immune to the (In)GaAs substrates [35], but not entirely unaffected at the Ge substrate; the ALD operating in high pressure generates similar concerns for the oxygen residual. The established records of initial O_2 adsorption on Ge(001) have made their comments based on the very first work by Fukuda and Ogina two decades ago, who suggested that one of the dissociated O atoms of O_2 sits at the bridge site and the other at a backbond of the Ge-Ge dimer [34,36]. However, the nondissociative O_2 adsorption have also been experimentally and theoretically proposed later in the literature [33,37,38]. Nevertheless, the established records fall short of experimental investigations on the interfacial electronic structure of Ge(001) with atomic O and molecular O_2, especially at the embryonic stage of adsorption. Worse yet, the investigations on an *epi* Ge(001)-2×1 surface are practically non-existed in the literature, the lack of which blinds us from improving the growth processes.

In this work, *epi* Ge(001)-2×1 samples were exposed to atomic oxygen as well as high-purity O_2 at dosages from as small as 0.06 Langmuir (L) to as high as 400 L. The O/Ge systems were probed by SRPES, which has been manifested as a superb tool to probe the atom-to-atom interactions at the interface. The tunability of photon energies allows us to acquire the spectra with high surface sensitivity, not to be realized by the conventional X-ray spectroscopy (XPS). Note that the present work does not deny the established XPS works because at its resolution, it is not possible to trace a surface component with a line shift from the bulk as small as 150 meV. The shallow Ge 3d core-levels with the binding energies smaller than 20 eV could provide rich bonding information and only SRPES could accommodate it with high signal-to-noise ratio and the high-resolution data reserve the small feature not to be escaped from detection. At a low concentration, we can trace the response of each atom in a buckled dimer to oxygen in the atomic form. It was surprising to observe that only the charge-enriched up-dimer atom allows the atomic O in the vicinity, while the down-dimer atom is inert to oxygen. Furthermore, the up-dimer atom generously donates its excess charge to the bonded oxygen atom under the intact dimer bond in the atomic-O exposure. Consequently, the charge environment becomes similar to that of the down-dimer atom. For O_2/Ge(001), we found that only the charge-enriched up-dimer atoms incline to accept O into the vicinity, whereas the charge-deficient down-dimer atoms remain inert to O. Two oxygen-induced chemical states are resolved at approximately 0.31 and 1.20 eV below the bulk component at 1 L, suggesting an immediate etching effect of O_2 to the surface dimers. The present experimental result provides direct evidence that the unpassivated down-dimer atoms may be a mechanism explaining the reliability issue related to Ge MOS devices [39,40].

2. Materials and Methods

2.1. sample preparations

The MBE technique was used to grow *epi* Ge(001)-2×1 layers on a Ge substrate. Sb-doped n-type Ge(001) wafer with a resistivity of 0.31–0.34 Ω-cm was dipped in 2% diluted HF solution and rinsed in de-ionized water. The wafer was then immediately loaded into a multi-chamber MBE/analysis system [41], in which it was annealed in a UHV at 600°C for 20 min to achieve an ordered surface. The quality of the sample was assessed based upon the streaky reconstructed reflection high-energy electron diffraction (RHEED) patterns [42]. Next, 7-nm thick Ge was grown on the annealed Ge substrate using an effusion cell in an MBE chamber at a UHV pressure of less than of 2×10^{-10} Torr. Using this approach, the Ge epi-layer shows a greatly improved 2× RHEED pattern with streaky diffraction spots and more distinct Kikuchi arcs. The sharper and more intense diffraction patterns indicate the attainment of a morphologically flatter and atomically more ordered surface [2]. The samples were stored *in vacuo* in a portable UHV module to transport to the nearby National Synchrotron Radiation Research Center for SRPES measurements. Photoelectrons were collected

with a 150-mm hemispherical analyzer (SPECS, GmbH) in a μ-metal chamber with a base pressure better than 1.2×10^{-10} Torr. The overall instrumental resolution was greater than 60 meV. The energy reference was determined using a silver film freshly grown from an electron gun prior to the measurements. Atomic oxygen was generated through a commercial cracker (SPECS, GmbH), and the dosage (L) was determined by the length of time on cracking and the chamber pressure.

2.2. data analysis

The objective of SRPES experiments on semiconductor surfaces is to relate the observable features with the known properties of the reconstructed surfaces. A photoemission component is commonly represented by a Voigt function line; that is, it is a convolute of Lorentzian and Gaussian functions. A model function assumed to consist of a multiplicity of overlapping components should be set up and fit accordingly to the data by the method of least squares. Constraints are necessary in order to reduce the ambiguity of a fit, such as the lifetime width and spin-orbit splitting and ratio essentially identical for all components. Three parameters are for each spin-orbit pair, its position, height, and Gaussian width. The amplitude of the line is in principle related to the areal density and location of the atoms within the surface layer through the inelastic mean-free path (IMFP), assuming that the experimental intensity is not compromised by diffraction. Since the areas of Voigt function lines are not proportional to the product of peak height and Gaussian width, it will be necessary to numerically integrate the area in order to set the peak amplitude. In the buckled dimer reconstruction of the Ge(100) surface, each layer contains an equal number of atoms. Those in the surface layer exist in two states in equal number. In Si(001), there are features that divide the atoms in both the first and second subsurface layers into two classes. See Fig. 1. However, the atoms in the second subsurface layer have been considered to be identical in Ge(001) in contrast to the case in Si(001). In other words, only the first two top surface layers of Ge(001) are regarded to behave differently from the bulk.

The algorithm that has been successfully set up to keenly analyze the much complicated line shape of the Si 2p core-level spectrum will be mainly used here to approach the Ge 3d core-level spectra. The details can be found elsewhere [20,21]. In brief, assumption of the layerwise attenuation through the parameters of the escape depth (λ) and the layer spacing (d) correlated by $x = \exp(-d/\lambda)$ gives the fractional areal strengths of the first and second layers to be $1 - x$ and $x^*(1-x)$, respectively. Given that the λ value is approximately 4 Å at a photon energy of 80 eV, the relative areal intensities, in the fit, of the first layer (S1), the second layer (S2), and the bulk (B) in the normal-emission spectrum are expected to be 28%, 24%, and 48%, respectively. Because the layerwise attenuation models estimated the maximum fractional intensity of the second layer is only 0.24, an unconstrained model function that gives a larger fractional intensity for the second layer can be immediately discarded.

3. Results and discussion

3.1. clean epi Ge(001)-2×1 surface

The surface atoms naturally exhibit electronic structures distinct from the bulk atoms. Core-level photoemission is highly sensitive to the surface electronic structure, which is manifested by a line shift from the bulk. The magnitude is commonly called as a surface core-level shift (SCLS). If the surface line lies in a lower binding energy than the bulk, the shift is conventionally regarded as a negative shift, if higher, the shift is said a positive shift. In the specific Ge studies, efforts have been made on the interpretation of the shallow Ge 3d core-level spectrum [22,43-47]. The lack of a consensus in the SCLSs of the dimerized surface atoms in the established reports is rather unusual, despite the similar line shapes in these room-temperature data and fewer contributed line components in Ge 3d state than those in the Si 2p state [21,44]. Some suggested that the dimers are unbuckled, thereby giving rise to only one S1 component in the spectra [43]. The proposal for a dimerized surface claimed differently in the shifted sign of the down atoms with a positive shift [43-45] and no shift at all [46,47]. Not only the surface component(s) has been claimed differently in various research groups, the line position of the second surface layer has also disagreed between groups with suggestion of a positive [22] or a negative shift [43-47]. As follows, we show a resolution

by approaching the line shape of an *epi* Ge(001)-2×1 surface assisted with the physical IMFP effect. Note that the existed reports mentioned above dealt with chemically treated surfaces.

Figure 2(a) displays SRPES-acquired *epi* Ge 3d core-level spectra in normal and 65° off-normal emission at room temperature. It is worth mentioning that the data presented in Fig. 2 were collected after the samples had been in the portable UHV module for 48 hrs. The absence of an oxidation state suggests that the *epi* Ge(001) surface is rather stable in vacuum. If a similar arrangement is applied to Si(001), the surface dangling bonds will certainly be oxidized.

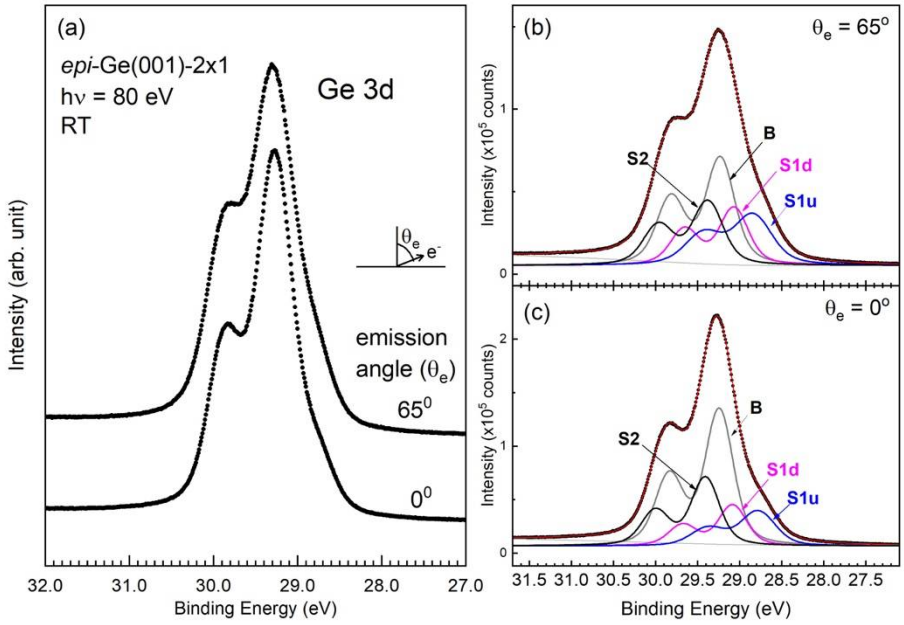

Figure 2. (a) Photoemission data from as-grown *epi* Ge(001)-2×1 taken in normal (θ_e = 0º) and off-normal (θ_e = 65º) emission at photon energies (hν) = 80 eV at room temperature. **(b)** A simultaneous fit to the 65º-emission spectrum. **(c)** A simultaneous fit to the normal-emission spectrum.

As shown in Fig. 2(a), a component lies clearly on the low-energy shoulder of the bulk component. Moreover, the change in line shape with emission angles is also observed, which is in contrast to the literature that reported little change in spectral line shape at different energies and emission angles [22,44-46]. Namely, the valley region increases in strength with increasing emission angles. Clearly, the *epi* Ge(001) surface shows a distinct surface electronic structure by SRPES that cannot be overlooked upon dielectric deposition. Note that the acquired XPS spectrum becomes broadened due to poor energy resolution, and the IMFP effect renders the contribution of surface emission rather small (data not shown).

Evidently, a fit is necessary to clearly extract the embedded components of the *epi* Ge 3d line shape. A preliminary analysis using a proper model function suggests the need of four Voigt function-like components, which reside on a parameterized background and separate energy-loss tail. The background is represented by four parameters: a constant, a slope, and a two-parameter power-law. This background function successfully represents the degraded electron from a shallow Ge 3d level, where the loss tail is due to the electron-hole pair excitations in the spectral energy range. The presence of such a tail does not affect the primary line structure because the onset of electron-hole pair excitations commences at 1.2 eV away from the bulk line. Note that the background function must be incorporated in a fit. Subtraction of the background prior to a fit should be avoided, because it ignores the physical electron-hole pair excitations.

A representative fit to the room-temperature data is plotted in Figs. 2(b) and (c) for θ_e = 65° and 0°, respectively. In this fit, the spin-orbit splitting is 0.593, and the spin-orbit branching ratio varies greatly from 0.514 in normal emission to 0.626 in θ_e = 65°. The lifetime width is 0.172 eV. The small branching ratio has been reasoned as the nearness of the photon energy to the photoemission threshold [48,49]. The binding energy of the bulk Ge 3d state is resolved at 29.25 eV. The SCLSs of the

S1u, S1d, and S2 components are −0.462, −0.159, and +0.165 eV in the normal emission, respectively. The S2 component is nothing but originating from the second surface layer [20,22]. The resultant intensities of the three surface components follow the expectation from the IMFP effect.

Decades of researches on Si(001)-2×1 and Ge(001)-2×1 came to the consensus that the final-state theory explains the Si 2p and Ge 3d core-level spectra better than the initial-state theory. The final-state picture includes a crystal ensemble with a created core hole and a photo-excited electron. Pehlke and Scheffler [50] calculated the final-state values for the S1u and S1d components to be −0.67 and −0.39 eV away from the bulk, respectively. For one's reference, the initial-state values for the S1u and S1d components were −0.50 and +0.27 eV, respectively. Apparently, a large screening shift was found for the 3d core electrons emitted from the down-dimer atoms. This was hypothesized to be the unoccupied dangling-bond state contributed by down-dimer atoms pulled down because of the influence from a core hole. The down-shifted dangling-bond state becomes populated by electrons from the Fermi level, thereby giving rise to effective screening. The under value found in the present work suggests imperfect screening in the physical process [50]. Note that the phenomenon is less apparent in the 3d core electrons from the up-dimer atoms because the corresponding dangling-bond state is already occupied. The final-state model predicts that the SCLS of the S2 component is negative in line position [50,51], which disagrees with the results presented in Fig. 2(a).

3.2. adsorption of molecular oxygen on epi Ge(001)-2×1 surface

The Ge 3d core-level spectra with various dosages of O_2 on the *epi* Ge(001)-2×1 surface at room temperature are shown in Fig. 3(a) taken with a 80 eV photon energy in normal emission. The inset plots the O 1s core-level spectra with selective O_2 dosages, where two O 1s states, O(I) and O(II), are clearly resolved 1 eV apart. As displayed in Fig. 3(a), adsorption of O_2 alters not drastically the line shape of the Ge 3d state, and development of a germanium-oxide state on the high binding energy side of the bulk state is not as significantly as that of SiO_x in Si(001)-2×1. The latter shows equally spaced peaks that gradually increase in intensity with increasing O_2 dosage [24]. The molecular oxygen affects immediately the S1u component in Fig. 3, suggesting that the oxygen clearly makes direct contact with the up-dimer atoms. As can be seen in Fig. 3(a), emission from the S1u state becomes broadened but still remains observable at great coverages. Clearly, attempt to have O_2 covering all the surface-dimerized atoms is unlikely, even 1000 L of O_2 exposure is of little help here [52]. In other words, the O_2/Ge(001)-2×1 interface is unlikely to breed up high-oxidation states. In comparison, merely 10 L of O_2 on Si(001)-2×1 have already developed four oxidation states with the highest one at the surface region and the smallest one on the bottom of the oxide layer [24]. Note that the surface Si-Si dimers remain detectable at 10 L of O_2 dosage, suggesting the local distribution of the SiO_x.

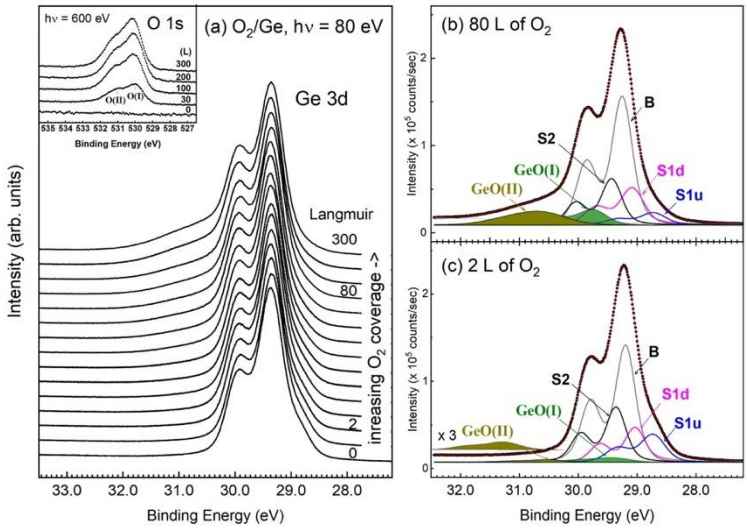

Figure 3. (**a**) The Ge 3d core-level spectra with various dosages of O_2 on an *epi* Ge(001)-2×1 surface at room temperature; (**b**) a fit to the Ge 3d core-level spectrum with 80 L of O_2 on Ge(001)-2×1; (**c**) a fit to the Ge 3d core-level spectrum with 2 L of O_2 on Ge(001)-2×1.

The affected Ge atoms would either appear as an induced component in the spectra, or be removed from the surface. The induced Ge-O component would show an increased binding energy below the bulk component, which is embedded in the spectral line envelope. Other than the intruded feature lying an eV from the bulk line, another component sitting in the valley region is realized if the spectra of Fig. 3(a) are grouped together in the bulk line normalized to a constant height. Hence, six components are needed to represent the Ge 3d core-level spectra in the model function, 4 for the O_2-free and 2 for O_2-affected atoms. The number of O_2-induced components is consistent with two O 1s states as shown in the inset of Fig. 3(a).

A further analysis in line shape with a fit would allow us to realize the contacted oxygen to be in atomic or molecular form. Figures 3(b) and 3(c) display a fit to the 80 L and 2 L curves of Fig. 3(a), respectively. The induced GeO(I) and GeO(II) components are respectively resolved at approximately +0.355 and +1.333 eV, which gradually increase in intensity with increasing O_2 dosages. One might question the necessity of the GeO(I) component in Fig. 3(c) because its intensity is rather small. Were the GeO(I) component excluded in the model function, the S1d component would end up with an unphysical enhancement in intensity (~ 20%). The appearance of the GeO(I) component in the embryo stage of O_2 adsorption suggests the immediate attachment of O_2 onto the up-atom dimers upon arriving at the Ge(001) surface. That is to say, no mediate stage exists in the O_2 adsorption on Ge(001). In a fit, the S2 as well as the S1u component shows a gradual decrease in intensity with O_2 dosages.

In a separate experiment, deposition of a high-κ dielectric oxide onto the present 300-L O_2/Ge(001) surface has cleansed off a great amount of the GeO(II) component, which has a behavior similar to that of GaAs(001). That is to say, the GeO(II) is not an interfacial O/Ge component. The phenomenon clearly indicates that the Ge atoms in GeO(II) are those originated at the S1u up-dimer atoms now being set free to become the GeO(II) film. Once a S1u atom is freed, the other dissociated O atom immediately fills the vacancy and bonds with the S2 atom underneath, thereby giving rise to the GeO(I) component. As shown in Figs. 3(b) and (c), the S1d component remains virtually in the same areal intensity as in the clean surface, which suggests that it does not follow the reacted pathway of the S1u component. Figure 4(a) presents the schematic drawings that summarize the interaction of O_2 with an up-dimer atom. The drawing is self-explanatory that the incoming molecular oxygen would encounter a disruption of the Ge-Ge dimer so that one of them would remove the up-dimer atom and the other immediately bonds with the nearby underneath subsurface Ge atom.

The preferential inclination of the O_2 molecules onto the up-dimer Ge atoms is certainly not found in the silicon counterpart and the previous reports of the chemically treated Ge surfaces [33,34,36,37]. On the one hand, the non-dissociative model should be forsaken because it would result in only one GeO and one O 1s component. The O_2-dissociative model, on the other hand, claimed non-destructive effect to the Ge-Ge dimers with one oxygen atom sitting at the top bridge site and the other the backbond of the surface dimer. This assignment meets fundamental difficulty that the bridged O would revert the buckled dimer to a symmetric configuration, and a change in the work function should be consequently observed because of the change of the dipole within the dimerized atoms. Our separate measurements of the valence-band spectra and the cutoff region show gradual increases of the O 2s state and an unshifted zero kinetic-energy point with various O_2 exposures, respectively. The latter indicates that the work function of the O_2/Ge interface stays at the same value as that of the clean surface. Moreover, it is known that the distribution of the Ge charge state in an oxide film would run less in the bulk than in the surface [24,53].

Peer-reviewed version available at Nanomaterials 2019, 9, 554; doi:10.3390/nano9040554

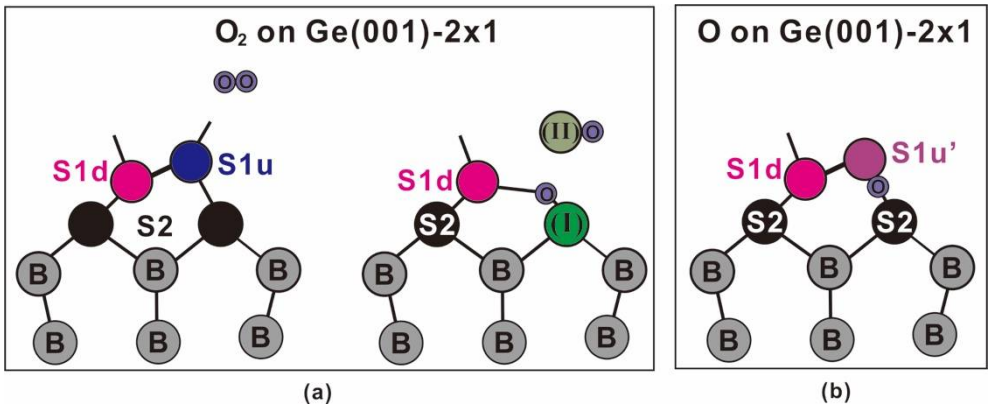

Figure 4. Schematic drawings of (**a**) O_2 onto Ge(001)-2×1, and (**b**) atomic O on Ge(001)-2×1 bonding configuration.

3.3. adsorption of atomic oxygen on epi Ge(001)-2×1 surface

Figure 5 displays a series of atomic-O covered *epi* Ge 3d core-level spectra taken with 80 eV photons at normal emission at room temperature. The dense plots in the bottom part of Fig. 5 are the result of finely incremental O dosages below 1.86 L, and the curves over a dosage of 50 L of dosages are shown in the upper part of the figure. As can be seen in Fig. 5, a gradual decrease in the surface intensity of the S1u state with increasing atomic O coverages suggests an immediate affiliation of the oxygen atoms with the surface dimers. As can be seen in Fig. 5, the 400-L spectrum is not significantly different from the 1.86-L spectrum, suggesting that the growth of atomic O on *epi* Ge(001)-2×1 is a self-limiting process. Furthermore, the Ge 3d spectra display a peak shift of 40 meV towards a lower binding energy upon the early appearance of oxygen atoms, which is later compensated for when the surface dimers have adsorbed the maximal amount of atomic O.

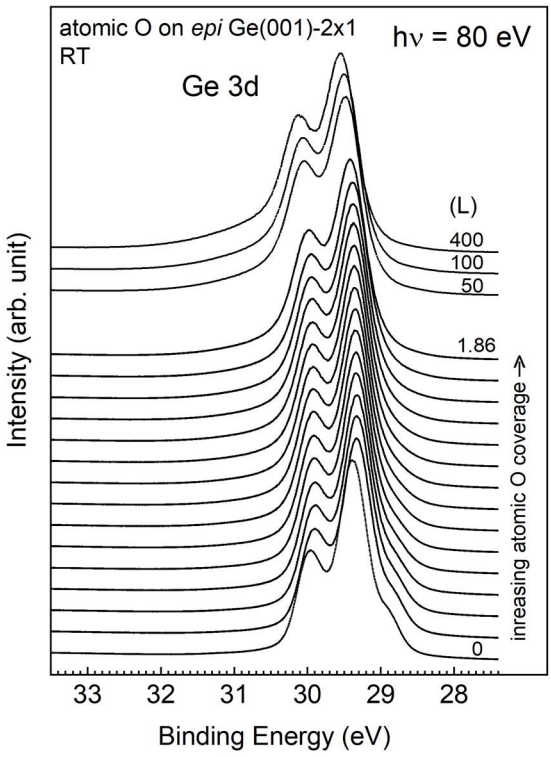

Figure 5. Development of the Ge 3d core-level spectra with various dosages of atomic O on an *epi* Ge(001)-2×1 surface at room temperature.

Figure 6 displays a fit for the representative curves in Fig. 5. Upon the early appearance of atomic O on the *epi* Ge(001)-2×1 surface, the line shape shows no great difference from the that of the clean surface. Hence, we employ the model function of the clean surface to analyze the O-affected line spectra with great success. In contrast to the case of O_2 on Ge(001)-2×1 above, the O-bonded Ge atoms do not occur in an energy position lower than the bulk atoms, but appear on the two dimer-related components. Note that the increased binding energy under expectation should be in reference to the S1u component. As can be seen in Fig. 6, the (S1u'+S1d) component gradually increases in strength at the expense of the S1u component. Moreover, the S2 component remains virtually unaltered in intensity even after the 400 L exposure to atomic oxygen (data not shown). Clearly, the O atoms confine the reaction to the topmost surface layer, and even restrict themselves to the top of the up-dimer atoms (see later). The oxidation path of atomic O on Ge(001)-2×1 certainly develops on its own, and it does not behaves similarly to that of O_2 on Si(001)-2×1 as well as on Ge(001)-2×1. Oxygen is readily available to accept full charge from Si in order to allow the interface to form a SiO_x film with x = 1 to 4 [24]. However, only a partial charge of the Ge surface atoms is needed to go to the adsorbed oxygen atoms.

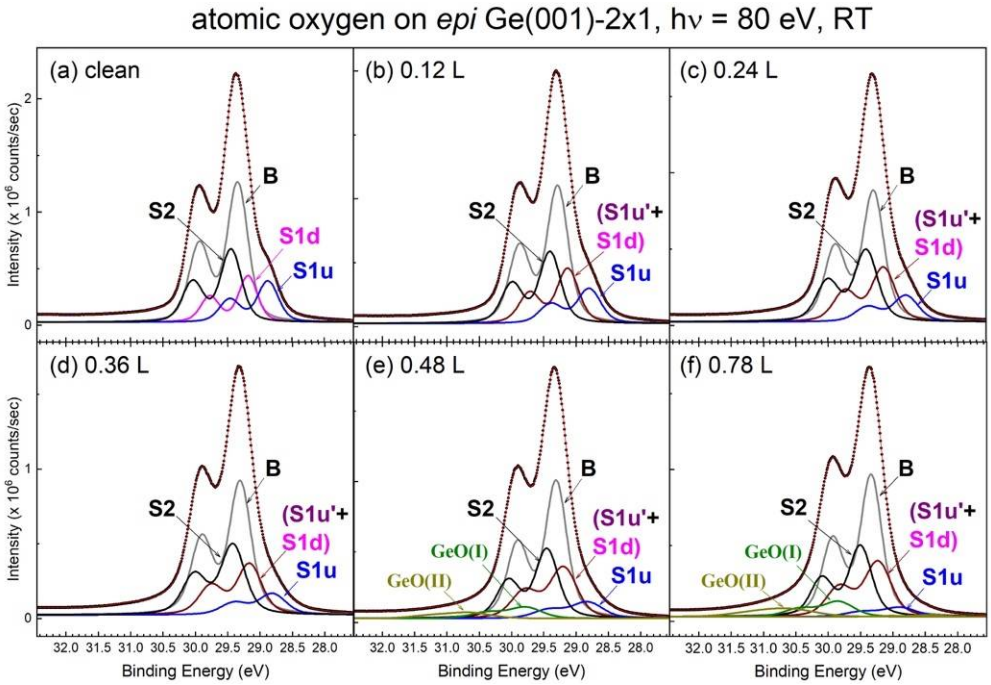

Figure 6. A fit to the representative Ge 3d core core-level spectra in Fig. 5 emphasizing the initially low atomic-O coverages.

As the (S1u'+ S1d) symbol suggests, it consists of two states, the S1d atoms and the other from the O-bonded S1u atoms (S1u'), which let the component 50% wider (e.g., 0.48 L) than the S1d component in the clean surface. The O-bonded S1u component appears fairly close to the S1d component in terms of energy position, thereby doubling the line intensity in the region. Attempts to split the S' component into two components yield too small of an intensity in the induced S1u component. Direct evidence to supporting this speculation drives from the information provided by the surface dipole. As is known, the buckled dimer has encountered a charge transfer from the down-dimer atom to the up-dimer atom, thereby giving rise to a dipole moment oriented with the positive end inwards in the asymmetric dimer. This will lead to an increase in the ionization potential (IP) of the buckled surface when compared with the unbuckled Ge(001)-2×1 surface. The change in IP upon O adsorption suggests an induced dipole. Because the atomic oxygen accepts charge from the up-dimer atom, the positive end of the O-Ge dipole moment orients the Ge atom. As a result, the IP becomes large in magnitude when the O atom resides on the up-dimer atom. The IP in a semiconductor is determined through the measurement of the spectral width (W) at a given photon

energy (hν). The former W is the energy separation of the valence band maximum (VBM) and the cutoff of the photo-ejected electrons. The IP value is directly determined without any assumption by subtracting hν from W [54,55].

Figure 7 plots the spectral development of the cutoff and valence band regions. As shown in Fig. 7, the onset of the cutoff moves gradually towards lower kinetic energies with increasing atomic O dosages. Extrapolation of the rising slope with the constant background line pins down the cutoff position, and the IP development of each dosage with the nearly fixed valence band maximum (VBM) is plotted in the inset of Fig. 7. The IP value decreases from 5.31 eV in the clean surface to 5.02 eV after 0.78 L of atomic O dosage. The result of the decreased IP is contrary to the expectation that the O atom is above the Ge atom. Note that the final IP occurs when the atomic O bonds with the up-dimer atoms fully. Although the binding energies of component S1u' and S1d are close to each other, the O-bonded dimer is still manifested in the buckled orientation. The placement of the atomic O at the backbond site is in accordance with the upward dipole direction found in the present study as well as the theoretical calculation [56]. In the latter, it has been claimed that the highest energy-occupied surface states were exclusively backbond states [56]. The schematic drawing of atomic O/Ge(001)-2×1 bonding configuration is shown in Fig. 4(b). As shown in Figs. 6(e) and (f), the GeO(I) and GeO(II) components begin to appear at the Ge(001) surface, meaning that the O_2 has come into play on adsorption. It is because that the present setup for breaking the molecular oxygen into its atomic form is not 100% efficient according to the mass spectrum shown in the residual gas analyzer. However, the small O_2 residual does not affect the IP of the system as mentioned above.

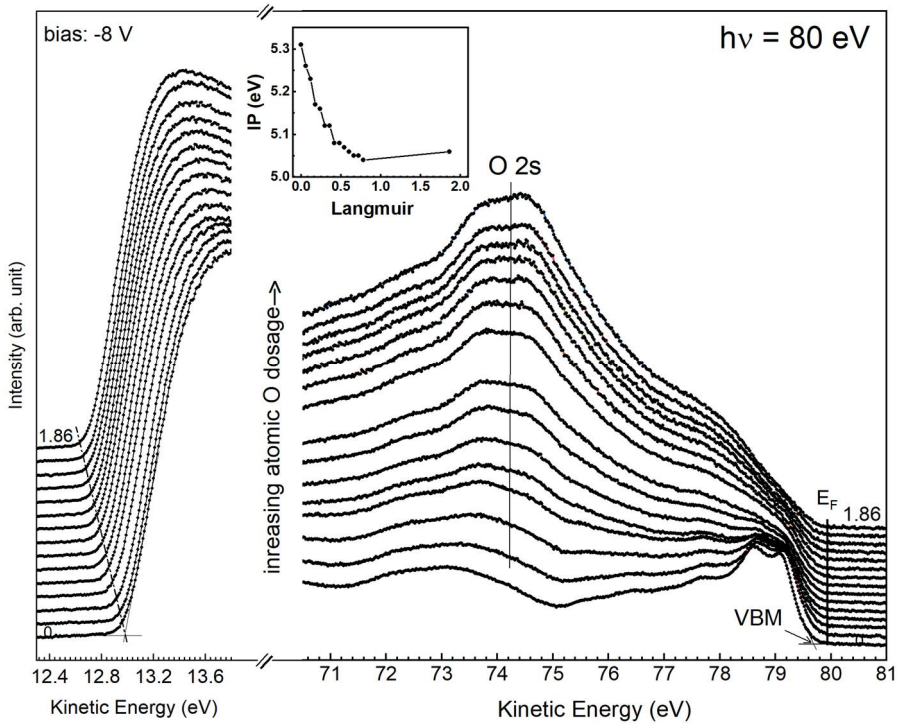

Figure 7. The acquired valence-band and cutoff spectra taken with a 80 eV photon energy with various atomic-O coverages. The inset shows the change of the ionization potential (IP).

As can be seen in Fig. 6, both the S1d and S2 components maintain the original energy positions with the unchanged SCLS signs in the atomic O-covered spectra. This suggests that the topmost dimers layer serves as a charge-enriched layer, while the subsurface layer serves as a charge-deficient layer. This indicates that a charge redistribution occurs between the first two surface layers. If this is indeed the case, the Ge 3d core-level spectra faithfully show that the sign of the shift is negative in the first surface layer and positive in the second surface layer. That is to say, a simple initial-state effect is sufficient to explain the spectral behavior.

4. Conclusions

An early stage of oxidation of an *epi* Ge(001)-2×1 surface by atomic as well as molecular oxygen is presented using high-resolution synchrotron radiation photoemission as a probe at room temperature. The pristine reconstructed Ge(001)-2×1 surface was firstly presented by setting up a proper model function to analyze the Ge 3d core-level spectrum, which is a must move for later observation of oxidation development. As a matter of fact, only the first two top surface layers are considered to behave distinctly from the bulk. The topmost surface, however, is buckled with one atom moving upwardly and the other downwardly. A charge transfer indeed occurs in between with the up-dimer atom being in a charge-enriched state, and the down-dimer atom a charge-deficient state. The charge environment plays a significant role for the oxygen atoms to preferentially react with the up-dimer atoms. For O_2, it is immediately dissociated without a mediated stage and simultaneously causes the up-dimer atom removed from the dimerized state. A dissociated oxygen bonds with the freed Ge atom, and the other inclines to be positioned at the site of the freed up-dimer atom, and bonds with the underneath Ge atom in the subsurface layer. The down-dimer atoms and those in the subsurface layer are inert to O_2. For atomic O, it selectively sits at the position between the up-dimer atom and the atom in the subsurface layer without causing a bond to be broken. Similar to the O_2 case, the down-dimer atoms are resistant to the effect of atomic oxygen. The reconstructed 2×1 configuration remains intact upon atomic O adsorption. Unlike the O/Si case, the adsorbed oxygen atoms accept partial charge from the contacted Ge atoms. Full coverage of the up-dimers atoms with oxygen renders the surface layer into a uniformly electronic state with excess charge. The second surface layer stays in the electronic state with a deficient charge. The present experimental results may explain some of the reliability problems associated with the Ge MOS devices.

Author Contributions: Minghwei Hong and Jueinai Kwo supervised the project. Yi-Ting Cheng acquired the SRPES data, and plotted the valence band spectra. Hsien-Wen Wan grew the *epi* Ge(001)-2×1 samples. Tun-Wen Pi did the fit and wrote the manuscript. All the authors revised the manuscript with eminent inputs from Chiu-Ping Cheng on the interpretation of the ionization potential. All the authors approved the final version of the manuscript.

Funding: This work was supported by MOST 105-2112-M-213-007-MY3, 105-2112-M-007-014-MY3, 107-2119-M-002-049-, 107-2923-M-002-003-, and 107-2622-8-002-018 of the Ministry of Science and Technology in Taiwan.

Conflict of Interest: The authors declare no conflict of interest.

References:

1. Chu, L.K.; Chu, R.L.; Lin, T.D.; Lee, W.C.; Lin, C.A.; Huang, M.L.; Lee, Y.J.; Kwo, J.; Hong, M. Effective passivation and high-performance metal-oxide-semiconductor devices using ultra-high-vacuum deposited high-κ dielectrics on Ge without interfacial layers. *Solid-State Electron.* **2010**, *54*, 965.
2. Chu, R.L.; Liu, Y.C.; Lee, W.C.; Lin, T.D.; Huang, M.L.; Pi, T.W.; Kwo, J.; Hong, M. Greatly improved interfacial passivation of *in-situ* high κ dielectric deposition on freshly grown molecule beam epitaxy Ge epitaxial layer on Ge(100). *Appl. Phys. Lett.* **2014**, *104*, 202102.
3. Dimoulas, A.; Tsoutsou, D.; Galata, S.; Panayiotatos, Y.; Mavrou, G.; Golias, E. Ge surfaces and its passivation by rare earth lanthanum germanate dielectric. *ECS Trans.* **2010**, *33*, 433-446.
4. Hu, S.; McDaniel, M.D.; Posadas, A.; Hu, C.; Wu, H.; Yu, E.T.; Smith, D.J.; Demkov, A.A.; Ekerdt, J.G. Monolithic integration of perovskites on Ge(001) by atomic layer deposition: a case study with $SrHf_xTi_{1-x}O_3$. *MRS Communications* **2016**, *6*, 125-132.

5. Lu, C.; Lee, C.H.; Zhang, W.; Nishimura, T.; Nagashio, K.; Toriumi, A. Structural and thermodynamic consideration of metal oxide doped GeO_2 for gate stack formation on germanium. *J. Appl. Phys.* **2014**, *116*, 174103.
6. Pourtois, G.; Houssa, M.; Delabie, A.; Conard, T.; Caymax, M.; Meuris, M.; Heyns, M.M. Ge 3d core-level shifts at (100)Ge/Ge(Hf)O_2 interfaces: A first-principles investigation. *Appl. Phys. Lett.* **2008**, *92*, 032105.
7. Sun, J.; Lu, J. Interface Engineering and Gate Dielectric Engineering for High Performance Ge MOSFETs. *Adv. Cond. Matter Phys.* **2015**, *2015*, 639218.
8. Takagi, S.; Kim, S.H.; Yokoyama, M.; Nishi, K.; Zhang, R.; Takenaka, M. Material challenges and opportunities in Ge/III-V channel MOSFETs. *ECS Trans.* **2014**, *64*, 99-110.
9. Hong, M.; Kwo, J.; Lin, T.D.; Huang, M.L. InGaAs metal oxide semiconductor devices with $Ga_2O_3(Gd_2O_3)$ high-κ dielectrics for science and technology beyond Si CMOS. *MRS Bulletin* **2009**, *34*, 514-521.
10. Lin, T.D.; Chang, Y.H.; Lin, C.A.; Huang, M.L.; Lee, W.C.; Kwo, J.; Hong, M. Realization of high-quality HfO_2 on $In_{0.53}Ga_{0.47}As$ by *in-situ* atomic-layerdeposition. *Appl. Phys. Lett.* **2012**, *100*, 172110.
11. Hong, M.; Wan, H.W.; Lin, K.Y.; Chang, Y.C.; Chen, M.H.; Lin, Y.H.; Lin, T.D.; Pi, T.W.; Kwo, J. Perfecting the $Al_2O_3/In_{0.53}Ga_{0.47}As$ interfacial electronic structure in pushing metal-oxide-semiconductor field-effect-transistor device limits using *in-situ* atomic-layer-deposition. *Appl. Phys. Lett.* **2017**, *111*, 123502.
12. Lin, T.D.; Chiu, H.C.; Chang, P.; Tung, L.T.; Chen, C.P.; Hong, M.; Kwo, J.; Tsai, W.; Wang, Y.C. High-performance self-aligned inversion-channel $In_{0.53}Ga_{0.47}As$ metal-oxide-semiconductor field-effect-transistor with $Al_2O_3/Ga_2O_3(Gd_2O_3)$ as gate dielectrics. *Appl. Phys. Lett.* **2008**, *93*, 033516.
13. Ren, F.; Kuo, J.M.; Hong, M.; Hobson, W.S.; Lothian, J.R.; Lin, J.; Tsai, H.S.; Mannaerts, J.P.; Kwo, J.; Chu, S.N.G.; Chen, Y.K.; Cho, A.Y. $Ga_2O_3(Gd_2O_3)$/InGaAs enhancement-mode n-channel MOSFETs. *IEEE Electron Device Lett.* **1998**, *19*, 309-311.
14. Kim, H.; McIntyre, P.C.; Chui, C.O.; Saraswat, K.C.; Cho, M.-H. *Appl. Phys. Lett.* **2004**, *85*, 2902.
15. Lee, W.C.; Chin, B.H.; Chu, L.K.; Lin, T.D.; Lee, Y.J.; Tung, L.T.; Lee, C.H.; Hong, M.; Kwo, J. Molecular beam epitaxy-grown Al_2O_3/HfO_2 high-κ dielectrics for germanium. *J. Crystal Growth* **2009**, *311*, 2187-2190.
16. Chu, L.K.; Lin, T.D.; Huang, M.L.; Chu, R.L.; Chang, C.C.; Kwo, J.; Hong, M. $Ga_2O_3(Gd_2O_3)$ on Ge without interfacial layers: Energy-band parameters and metal oxide semiconductor devices. *Appl. Phys. Lett.* **2009**, *94*, 202108.
17. Delabie, A.; Bellenger, F.; Houssa, M.; Conard, T.; Elshocht, S.V.; Caymax, M.; Heyns, M.; Meuris, M. Effective electrical passivation of Ge(100) for high-κ gate dielectric layers using germanium oxide. *Appl. Phys. Lett.* **2007**, *91*, 082904.
18. Xie, Q.; Deng, S.; Schaekers, M.; Lin, D.; Caymax, M.; Delabie, A.; Jiang, Y.; Qu, X.; Dedutytsche, D.; Detavernier, C. *IEEE Electron Device Lett.* **2011**, *32*, 1656.
19. Lee, C.H.; Nishimura, T.; Nagashio, K.; Kita, K.; Toriumi, A. *IEEE Trans. Electron Devices* **2011**, *58*, 1295.
20. Pi, T.W.; Cheng, C.P.; Wertheim, G.K. The reaction of Si(001)-2×1 with magnasium. *J. Appl. Phys.* **2011**, *109*, 043701.
21. Pi, T.W.; Hong, I.H.; Cheng, C.P.; Wertheim, G.K. Surface photoemission from Si(100) and inelastic electron mean-free-path in silicon. *J. El. Spectr. Rel. Phen.* **2000**, *107*, 163-176.

22. Pi, T.W.; Wen, J.F.; Ouyang, C.P.; Wu, R.T. Surface core-level shifts of Ge(100)-2×1. *Phys. Rev. B* **2001**, *63*, 153310.
23. Sun, S.; Sun, Y.; Liu, Z.; Lee, D.I.; Peterson, S.; Pianetta, P. Surface termination and roughness of Ge(100) cleaned by HF and HCl solutions. *Appl. Phys. Lett.* **2006**, *88*, 021903
24. Pi, T.W.; Wen, J.F.; Ouyang, C.P.; Wu, R.T.; Wertheim, G.K. Oxidation of Si(001)-2×1. *Surf. Sci.* **2001**, *478*, L333-L338.
25. Wada, A.; Zhang, R.; Takagi, S.; Samukawa, S. Formation of thin germanium dioxide film with a high-quality interface using a direct neutral beam oxidation process. *Jpn. J. App. Phys.* **2012**, *51*, 125603.
26. Sahari, S.K.; Murakami, H.; Fujioka, T.; Bando, T.; Ohta, A.; Makihara, K.; Higashi, S.; Miyazaki, S. Native oxidation growth on Ge(111) and (100) surfaces. *Jpn. J. App. Phys.* **2011**, *50*, 04DA12.
27. Prabhakaran, K.; Maeda, F.; Watanabe, Y.; Ogino, T. Distinctly different thermal decomposition pathways of ultrathin oxide layer on Ge and Si surfaces. *Appl. Phys. Lett.* **2000**, *76*, 2244.
28. Milojevic, M.; Contreras-Guerrero, R.; Lopez-Lopez, M.; Kim, J.; Wallace, R.M. Characterization of the"clean-up" of the oxidized Ge(100) surface by atomic layer deposition. *Appl. Phys. Lett.* **2009**, *95*, 212902.
29. Molle, A.; Spiga, S.; M.Fanciulli. Stability and interface quality of GeO_2 films grown on Ge by atomic oxygen assisted deposition. *J. Chem. Phys.* **2008**, *129*, 011104.
30. Molle, A.; Bhuiyan, M.N.K.; Tallarida, G.; Fanciulli, M. In situ chemical and structural Investigations of the oxidation of Ge(001) substrates by atomic oxygen. *Appl. Phys. Lett.* **2006**, *89*, 083504.
31. Yoshigoe, A.; Teraoka, Y.; Okada, R.; Yamada, Y.; Sasaki, M. In situ synchrotron radiation photoelectron spectroscopy study of the oxidation of the Ge(001)-2×1 surface by supersonic molecular oxygen beams. *J. Chem. Phys.* **2014**, *141*, 174708.
32. Cho, J.H.; Kim, K.S.; Morikawa, Y. Structure and binding energies of unsaturated hydrocarbons on Si(001) and Ge(001). *J. Chem. Phys.* **2006**, *124*, 024716.
33. Fan, X.L.; Lau, W.M.; Liu, Z.F. Nondissociative Adsorption of O_2 on Ge(100). *J. Phys. Chem. C* **2009**, *113*, 8786-8793.
34. Fleischmann, C.; Schouteden, K.; Merckling, C.; Sioncke, S.; M. Meuris; Haesendonck, C.V.; Temst, K.; A.Vantomme. Adsorption of O_2 on Ge(100): Atomic Geometry and Site-Specific Electronic Structure. *J. Phys. Chem. C* **2012**, *116*, 9925-9929.
35. Pi, T.W.; Lin, Y.H.; Fanchiang, Y.T.; Chiang, T.H.; Wei, C.H.; Lin, Y.C.; Wertheim, G.K.; Kwo, J.; Hong, M. *In-situ* atomic layer deposition of tri-methylaluminum and water on prestine single-crystal (In)GaAs surfaces: electronic and electric structures. *Nanotechnology* **2015**, *26*, 164001.
36. Fukuda, T.; Ogino, T. Initial oxygen reaction on Ge(100)2×1 surfaces. *Phys. Rev. B* **1997**, *56*, 13190-13193.
37. Shah, G.A.; Radny, M.W.; Smith, P.V. Initial stages of oxygen chemisorption on the Ge(001) surface. *J. Phys. Chem. C* **2014**, *118*, 15795-15803.
38. Soon, J.M.; Lim, C.W.; Loh, K.P.; Ma, N.L.; Wu, P. Initial-stage oxidation mechanism of Ge(100)2×1 dimers. *Phys. Rev. B* **2005**, *72*, 115343.
39. Franco, J.; Kaczer, B.; Roussel, P.J.; Mitard, J.; Sioncke, S.; Witters, L.; Mertens, H.; Grasser, T.; Groeseneken, G. Understanding the suppresed charge trapping in relaxed- and strained-Ge/SiO_2/HfO_2 pMOSFETs and implications for the screening of alternative high-mobility substrate/dielectric CMOS gate stacks. *Proc. 2013 IEEE International Electronic Devices Meeting* **2013**, 358-362.

40. Wan, H.W.; Hong, Y.J.; Cheng, Y.T.; Kwo, J.; Hong, M. BTI Characterization of MBE Si-capped Ge Gate Stack and Defect Reduction via Forming Gas Annealing. *Proc. 2019 IEEE International Reliability Symposium* **2019** (accepted).
41. Lee, K.Y.; Lee, W.C.; Lee, Y.J.; Huang, M.L.; Chang, C.H.; Wu, T.B.; Hong, M.; Kwo, J. Molecular beam epitaxy grown template for subsequent atomic layer deposition of high κ dielectrics. *Appl. Phys. Lett.* **2006**, *89*, 222906.
42. Cheng, Y.T.; Lin, Y.H.; Chen, W.S.; Lin, K.Y.; Wan, H.W.; Cheng, C.P.; Cheng, H.H.; Kwo, J.; Hong, M.; Pi, T.W. Surface electronic structure of *epi* Germanium (001)-2×1. *Appl. Phys. Express* **2017**, *10*, 075701.
43. Cao, R.; Yang, X.; Terry, J.; Pianetta, P. Core-level shifts of the Ge(100)-(2×1) surface and their origins. *Phys. Rev. B* **1992**, *45*, 13749-13752.
44. Eriksson, P.E.J.; Uhrberg, R.I.G. Surface core-level shifts on clean Si(001) and Ge(001) studied with photoelectron spectroscopy and density functional theory calculations. *Phys. Rev. B* **2010**, *81*, 125443.
45. Goldoni, A.; Modesti, S.; Dhanak, V.R.; Sancrotti, M.; Santoni, A. Evidence for three surface components in the 3d core-level photoemission spectra of Ge(100)-(2×1) surface. *Phys. Rev. B* **1996**, *54*, 11340-11345.
46. Landemark, E.; Karlsson, C.J.; Johansson, L.S.O.; Uhrberg, R.I.G. Electronic structure of clean and hydrogen-chemisorbed Ge(001) surfaces studied by photoelectron spectroscopy. *Phys. Rev. B* **1994**, *49*, 16523-16533.
47. Le Lay, G.; Kanski, J.; Nilsson, P.O.; Karlsson, U.O.; Hricovini, K. Surface core-level shifts on Ge(100): c(4×2) to 2×1 and 1×1 phase transitions. *Phys. Rev. B* **1992**, *45*, 6692-6699.
48. Margaritondo, G.; Rowe, J.E.; Christman, S.B. Photoionization cross section of d-core levels in solids: A synchrotron radiation study of the spin-orbit branching ratio. *Phys. Rev. B* **1979**, *19*, 2850-2855.
49. Aarts, J.; Hoeven, A.-J.; Larsen, P.K. Core-level study of the phase transition on the Ge(111)-c(2×8) surface. *Phys. Rev. B* **1988**, *38*, 3925-3930.
50. Pehlke, E.; Scheffler, M. Evidence for site-sensitive screening of core holes at the Si and Ge (001) surface. *Phys. Rev. Lett.* **1993**, *71*, 2338-2341.
51. Binder, J.F.; Broqvist, P.; Komsa, H.; Pasquarello, A. Germanium core-level shifts at Ge/GeO_2 interfaces through hybrid functionals. *Phys. Rev. B* **2012**, *85*, 245305.
52. Schmeisser, D.; Schnell, R.D.; Bogen, A.; Himpsel, F.J.; Rieger, D.; Landgren, G.; Morar, J.F. Surface Oxidation States of Germanium. *Surf. Sci* **1986**, *172*, 455-465.
53. Houssa, M.; Pourtois, G.; Caymax, M.; Meuris, M.; Heyns, M.M. Electronic properties of (100)Ge/Ge(Hf)O_2 interfaces: A first-principles study *Surf. Sci.* **2008**, *602*, L25-L28.
54. Cheng, C.P.; Chen, W.S.; Lin, K.Y.; Wei, G.J.; Cheng, Y.T.; Lin, Y.H.; Wan, H.W.; Pi, T.W.; Tung, R.T.; Kwo, J.; Hong, M. Atomic nature of the Schottky barrier height formation of the Ag/GaAs(001)-2×4 interface: an *in-situ* synchrotron radiation photoemission study. *Appl. Surf. Sci.* **2017**, *393*, 294-298.
55. Kronik, L.; Shapira, Y. Surface photovoltage phenomena: theory, experiment, and applications. *Surf. Sci. Rep.* **1999**, *37*, 1-206.
56. Radny, M.W.; Shah, G.A.; Schofield, S.R.; Smith, P.V.; Curson, N.J. Valence Surface Electronic States on Ge(001). *Phys. Rev. Lett.* **2008**, *100*, 246807.